

# Improving antenna near-field pattern by use of artificial impedance screens

Stanislav Maslovski, Pekka Ikonen, *Student Member, IEEE*, Constantin Simovski, Mikko Kärkkäinen, Sergei Tretyakov, *Senior Member, IEEE*, and Vasil Denchev

**Abstract**—An antenna prototype utilizing artificial impedance surfaces to control the near field distribution is described. The antenna is a folded dipole placed above a finite-size artificial impedance surface. We have found that the field screening is most effective if the surface is a metal conductor. However, to achieve a reasonable value of the radiation resistance the dipole should be located far off the screen. If the surface is a magnetic wall, the antenna design is more compact, but the field behind the screen is large. Here we realize a compromise solution using an inductive surface of a moderate surface impedance, which allows realization of an effective near-field screen with still a reasonably low-profile design.

**Index Terms**—antenna, antenna near-field pattern, impedance surface, screening, antenna efficiency.

## I. INTRODUCTION

In paper [1] an idea of decreasing the field level on one side of low-profile antennas was proposed and developed. Using such antennas, efficiency can be maintained at a good level even if absorbing bodies are near the antenna but behind the screening substrate, because the power absorbed in the near vicinity of the antenna is reduced. The idea is based

Stanislav Maslovski, Pekka Ikonen, Mikko Kärkkäinen, and Sergei Tretyakov are with Radio Laboratory/SMARAD, Helsinki University of Technology, P.O. Box 3000, FIN-02015 HUT, Finland. Contact e-mail: stanislav.maslovski@hut.fi

Constantin Simovski is with Physics Dept. of the St. Petersburg State University of Information Technologies, Mechanics and Optics, 14 Sablinskaya str., 197101, Saint-Petersburg, Russia. Contact e-mail: simovsky@phd.ifmo.ru

on the usage of artificial impedance surfaces with moderate inductive impedances to form the desired near-field pattern of a horizontal antenna positioned parallel to the impedance surface. The known solutions for artificial antenna substrates (e.g., [2]) utilize impedance surfaces in the resonant regime (as artificial magnetic walls) in order to reduce the antenna thickness. In papers [2]–[5] implied applications of artificial impedance surfaces are within the resonant band. However, it has been shown in [1], [6] that the antenna solutions with a high inductive impedance of the ground surface do not correspond to a good screening effect in the near-zone field of horizontal antennas. The present approach allows an effective reduction of the near field behind the antenna, whereas the required radiation resistance can be achieved with a small increase of the structure thickness (the primary radiator antenna is positioned at a certain height over the impedance surface). Impedance screens of two kinds have been studied. The first one is so-called *mushroom* structure and the second one is a thin layer named *Jerusalem crosses* structure. These impedance screens should work well when the surface is of moderate inductive impedance and when the antenna excites mostly TE modes (respectively to the screen normal). In this work we validate experimentally our theoretical expectations designing optimized radiating elements for the use with two different impedance surfaces and measuring the near field distributions around the antenna. We do not study the far-field pattern since it is not a practically important characteristic

for handsets operating in the frequency range 1–2 GHz. Really, this pattern is weakly directive (because the antenna of a mobile phone is electrically small), and it is perturbed depending on the device position with respect to the user. However, the non-perturbed field distribution measured in the vicinity of a portable terminal clearly indicates the possible influence of the user body or other nearby located objects to the antenna. If the field behind the terminal (where the user's body is normally) is not significant, the user's body will not significantly reduce the antenna efficiency. Therefore, we make measurements at the distances of a few centimeters to test the near-field screening efficiency of the artificial impedance surface.

Notice, that in the known literature the problem of the improving the antenna efficiency and SAR reduction is often considered in terms of far-zone measurements and related with such a parameter of the antenna as the front-to-back ratio in the far zone. Following this point of view, if one wants to reduce the SAR one should form the far-zone antenna pattern with a small backward radiation [7], [8]. This is a potentially misleading approach. There is no proportionality between the far-zone and the near-zone field patterns, and a high front-to-back ratio for the far-zone fields can correspond to a small front-to-back ratio in the near zone. Only the measurements of the near-field spatial distribution (and not the field angular dependence since the angular near-field pattern strongly depends on the distance from the antenna) can definitely indicate the degree of field interactions between the antenna and various objects in its near field. Our measurements are, therefore, not conventional and they became possible due to the use of special equipment dedicated for near-field testing.

In the proposed design, the artificial impedance surface (such as the mushroom structure) is operating at frequencies below the surface impedance resonance, where the effective surface impedance is inductive and not high in the absolute

value. In this frequency range the surface supports TM-polarized surface waves, whose excitation is not desirable. This means that we should use a primary radiator that excites (at least primarily) TE-polarized waves, that is, there should be mainly electric currents parallel to the surface. A natural choice is a simple dipole antenna positioned parallel to the surface. Another choice criterion is the compact design. When a dipole antenna is brought close to a surface with a small inductive impedance, its radiation resistance becomes rather low due to cancelation of radiation from the currents induced on the surface. For this reason, a better choice is a folded dipole because of its high radiation resistance.

The use of a folded dipole requires a balun to connect the dipole to the unbalanced coaxial cable. At the first stages of our experiments we wanted to avoid complications related to any additional elements in the antenna system, and decided to use in experiments only a half of the dipole antenna (over a half of the artificial impedance surface) positioned orthogonal to a large metal ground plane. The mirror image of the half of the antenna simulates the other half, so that the whole system radiates as the complete antenna in the half space where the actual radiator is located. No balun is needed if the feeding cable is behind the ground plane because no currents are induced on the cable.

After successful tests with this installation, we designed a planar balun, manufactured and tested a complete antenna sample. Let us emphasize that our paper is not a description of a new practical antenna with good front-to-back ratio in the far field. The goal of this paper is to demonstrate the feasibility of handset antennas for the frequency range 1–2 GHz with reduced interaction with objects in the antenna near field region.

## II. MODELING MEASUREMENTS AND SIMULATIONS WITH ONE HALF OF THE ANTENNA STRUCTURE

### A. Experimental set-up

The experimental set-up modeling the complete antenna is shown in Figure 1. It consists of a  $220 \times 230 \text{ mm}^2$  rectangular metal screen with a 50 Ohm 3.5 mm coaxial connector in its center and a half of the antenna structure attached to the connector (and also to the screen, as explained below).

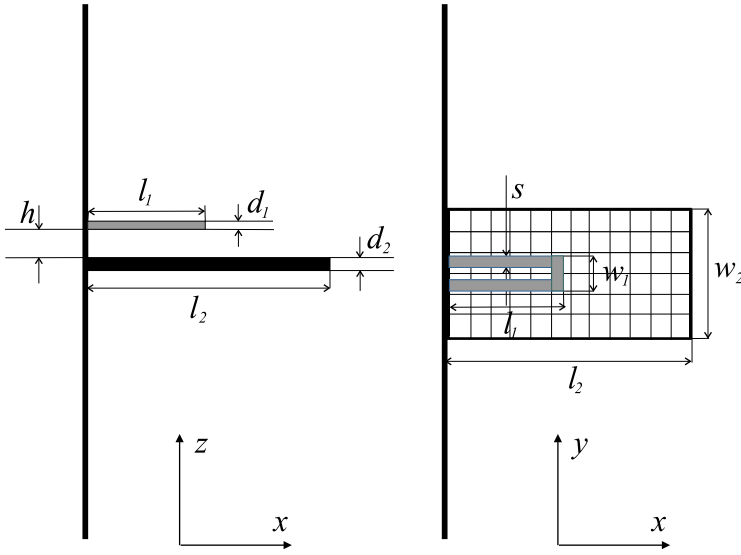


Fig. 1. Experimental modeling set-up: side view (left) and top view (right).

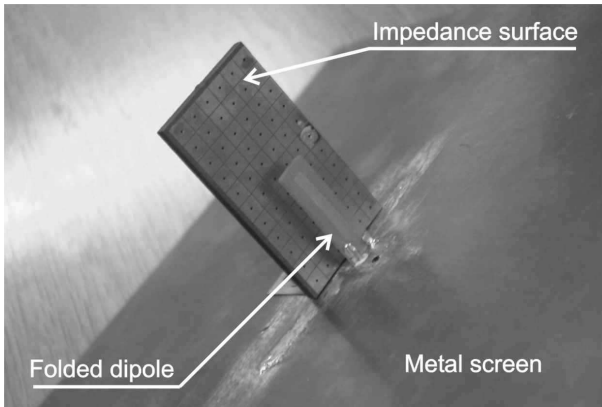


Fig. 2. Photo of the modeling set-up.

Neglecting the influence of the finite sizes of the screen and the effect of the finite screen conductivity, a half of the real antenna and its mirror image can be considered as forming the entire antenna. The source voltage (the source is represented

by the coaxial connector in our case) is then applied between the screen and one end of one half of the folded dipole. The second end of the dipole is connected to the ground (see Figure 2). The impedance surface should also be well electrically connected to the ground.

Cabling effects are eliminated here due to the simple fact that the cable is now behind the screen. It prevents currents from flowing on the outer surface of the coax. This means that there is no need for a special balancing device which can possibly influence the input impedance measurements, etc. The input impedance of the complete antenna is two times larger than that measured for a half of the antenna in this experimental set-up. The field distributions measured in this modeling set-up should correspond to the same distributions for the complete antenna in free space. The position of the impedance surface is adjustable mechanically, and the separation between the dipole and the surface can be changed. Three types of surfaces have been used in the experiments: a mushroom structure, a metal screen with slits shaped as Jerusalem crosses, and a simple metal screen, all of the same surface dimensions.

Antenna dimensions were chosen for operation around 1.8 GHz. To take into account the influence of the impedance screen on the effective resonant length of the antenna, measurements with a test microstrip transmission line formed above the impedance screen have been made. It was found that in the presence of the impedance surface the resonant length is slightly shorter than the same for the antenna in free space. It has been set approximately to 30 mm (it is the dipole half-length corresponding to the quarter wavelength distance). Folded dipole samples have been prepared from a metallized dielectric material (sheets of *FR-4*). Geometrical parameters for all studied cases (sizes are in mm, for the definition see Figure 1) are given in Table I. The last column gives the total thickness of the structures:  $H = d_1 + d_2 + h$ .

Distance  $h$  between the folded dipole and the impedance surface determines the input impedance of the antenna. The following experimental procedure to find an optimal distance was used. The working frequency was firstly chosen (close to 1.8 GHz). Then, the distance between the folded dipole and the impedance surface was changed until the imaginary part of the antenna input impedance became zero at the working frequency. If the real part of the impedance is close to 25 Ohm (note that in the modeling set-up we measure one half of the actual impedance of the complete antenna) for the same frequency, then the antenna is matched and ready for measurements. If this condition was not reachable, then a frequency close to the original one was chosen and the procedure was repeated.

TABLE I

DIMENSIONS OF THE ANTENNA ELEMENTS (IN MM).

	$l_1$	$l_2$	$d_1$	$d_2$	$h$	$w_1$	$w_2$	$s$	$H$
Mushrooms	33	62	1.6	3.3	4.6	9.0	32	3.0	9.5
Metal	33	62	1.5	0.45	7.4	10	30	3.2	9.35
Jerusalem crosses	33	60	1.5	0.80	10	10	33	3.2	12.3

### B. Impedance surfaces

Two designs of artificial impedance surfaces have been experimentally studied and compared with the case of a metal plate of the same size. The sizes of the impedance surfaces in both variants are indicated in Table I. Design 1 (mushroom structure) is an array of square metal patches on the upper surface of a metal-backed dielectric layer. The central points of every patch are connected to the ground plane by vertical vias. The theory of mushroom structures is well-known [3], [9]. The parameters of mushrooms and the dielectric layer (*Taconic TLY-5*) are shown in Figure 4. The surface impedance of this mushroom structure at  $f = 1.8$  GHz was theoretically estimated as  $Z_s \approx j50$  Ohm. We used the analytical theory from [9] which gives following approximate relations for a

simple mushroom structure:

$$Z_s \approx j \frac{\omega L}{1 - \omega^2 LC},$$

$$L = \mu_0 d_2, \quad C = \frac{D \epsilon_0 (\epsilon_r + 1)}{\pi} \log \frac{2D}{\pi \delta}, \quad lms \quad (1)$$

where  $d_2$  is the thickness of the mushroom structure,  $D$  is the patch array period and  $\delta$  is the gap between patches.

Notice, that a moderate inductive impedance is needed for the expected screening effect [1], [6], and the obtained result for  $Z_s$  fits to this condition. Design 2 (a screen with complex-shaped slits) is formed by a grid of slits made in a metal covering of a thin dielectric substrate (of the relative permittivity  $\epsilon_r = 4.5$ ). The thickness of the substrate is equal to 0.8 mm. The notations for all the dimensions of the slits are given in Figure 3. On this figure the slits in the metal screen are shown in black. The following sizes were chosen for the experimental sample:  $g = w = 0.2$  mm,  $d = 2$  mm,  $D = 4.2$  mm,  $h = 0.8$  mm. The theory of such surfaces is known for both cases when the substrate is metal-backed and when it is free [4], [5]. In our case it is free, and the surface impedance at low frequencies is complex with inductive imaginary part. It can be found as a parallel connection of the grid impedance of the slotted screen  $Z_g$  and the input impedance of the dielectric layer of thickness  $d_2$ :

$$Z_s = \frac{Z_d Z_g}{Z_d + Z_g}.$$

The grid impedance (relating the tangential electric field in the screen plane and the surface current induced on it) can be approximately presented as

$$Z_g \approx j \frac{\omega L_g}{1 - \omega^2 L_g C_g}, \quad lnew \quad (2)$$

and the dielectric layer in free space has the following surface impedance:

$$Z_d = \eta \frac{1 + \frac{j}{\sqrt{\epsilon_r}} \tan kd_2}{1 + j \sqrt{\epsilon_r} \tan kd_2}. \quad lnew1 \quad (3)$$

In new the effective inductance and capacitance determining the *grid* impedance of the uniplanar screen can be expressed

as

$$L_g = \frac{\mu_0 d}{\pi} \log \frac{2d}{\pi g}, \quad C_g = \frac{D \varepsilon_0 (\varepsilon_r + 1)}{\pi} \log \frac{2D}{\pi w}. \quad (4)$$

The notations are clear from Fig. 3. In new1  $k = \omega \sqrt{\varepsilon_0 \mu_0 \varepsilon_r}$  is the wave number of the dielectric medium. The real part of  $Z_s$  corresponds to the penetration of radiation through the impedance surface. For this design the analytically estimated surface impedance was  $Z_s \approx 0.80 + j17$  Ohm at 1.8 GHz.

This is also a moderate surface impedance.

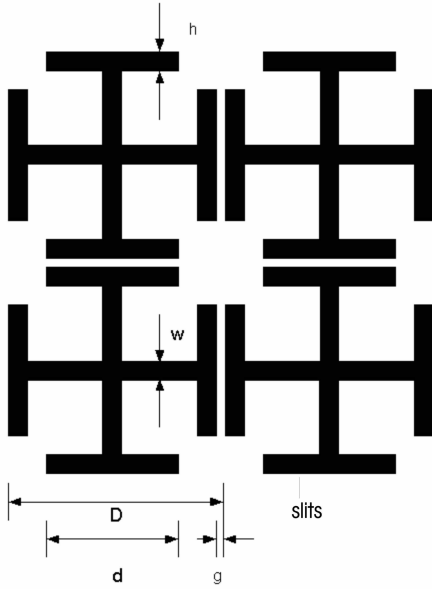


Fig. 3. A grid of slots shaped as Jerusalem crosses (slots are in black).

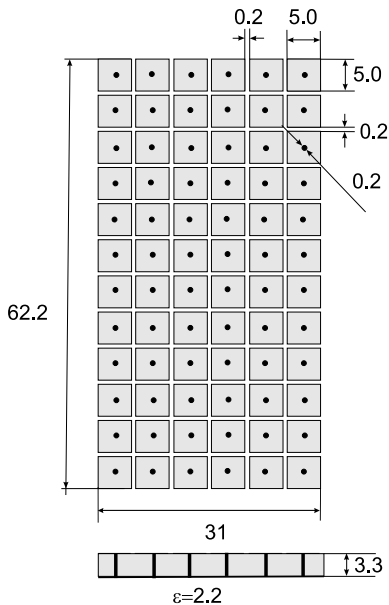


Fig. 4. Mushroom surface and dimensions of its elements (in mm).

To understand the influence of such impedance surfaces to the input parameters of the folded dipole we have calculated the wave impedance and the propagation constant of the infinite metal strip of width 3 – 4 mm raised at 5 – 10 mm over the impedance plane. This was done with the exact image method [10]. The results have shown no dramatic influence, and this has been confirmed by measurements.

### C. Measurements

Measurements with the modeling set-up have been done for a folded dipole above three types of impedance surfaces: metal surface, mushroom structure, and Jerusalem crosses structure. Near fields have been measured by a special set-up (proprietary design of SPEAG and HUT Radio Laboratory) developed for SAR measurements. The set-up has two probes, electric and magnetic, which allow measuring the *amplitudes* of three components of the field vectors. Unfortunately, the dipoles in the electric probe are oriented differently relatively to the usual laboratory coordinate system: They are *not* along the two horizontal directions and the vertical one. Because such components cannot be transformed to the usual ones without knowledge about the phases of the fields, the total absolute values of the field vectors have been measured.

At first, the near field distribution over the radiating folded dipole was measured, to check that the modeling antenna was operating in the desired regime and the field distribution corresponded to the expected pattern. The probe moved in a plane 7 mm above the half-dipole (here *above* corresponds to the orientation shown on Figure 1, left). The measurement points covered an area equal to the area of the underlying mushroom structure. The measurements showed that the electric near field had a maximum at the end of the half-dipole, and the magnetic field had its maximum close to the feeding point, as expected.

Next, we measured the distribution of the near field in vertical planes which included the antenna cross section. In the following series of measurements the probe was moved around

the antenna along a planar spiral path in the  $yOz$  plane (the axes are accordingly to Figure 1). The path covers an area of  $220 \times 230 \text{ mm}^2$ . The measurements have been performed at the antenna resonant frequency. The electric near field pattern of the folded dipole placed over the mushroom surface is depicted on Figure 5. Figure 6 shows the magnetic near-field distribution over the same plane. The field values are given in dB relatively to the maximum level. The coordinate axes are parallel to the edges of the ground plate. In these figures the plane over which the field distributions are measured is located in the middle of the half-dipole. The bottom side of the picture corresponds to the area behind the impedance surface where the screening effect is significant. The region  $0 < y < 70 \text{ mm}$ ,  $-40 \text{ mm} < z < 0$  should be excluded from the plots. This region was occupied by the antenna structure and it was impossible to move probes inside this area. As a result, we have measured the near field distribution inside a rather large spatial box containing the antenna except a small box having the sizes of the antenna itself.

We define the local screening effect (LSE) as the ratio (in dB) between the field amplitudes at two points located in front ( $z > 5 \text{ mm}$ ) and behind ( $z < -45 \text{ mm}$ ) the antenna structure, equidistantly from the antenna center. The averaged screening effect (ASE) is the averaged value of LSE over all these points covered by our measurements. For the mushroom structure ASE is approximately equal to 15 dB for electric fields and 20 dB for magnetic fields.

Next, we have studied the near-field patterns of a half of the folded dipole when the mushrooms are replaced by a metal surface and by the Jerusalem-crosses surface. The screening effect is maximal for the metal surface: ASE is close to 20 dB for both electric and magnetic fields. But for the input impedance of the half-dipole to be close to 25 Ohm, the metal screen should be positioned at a larger distance from the source than the mushroom layer (parameter  $h$  in Table I).

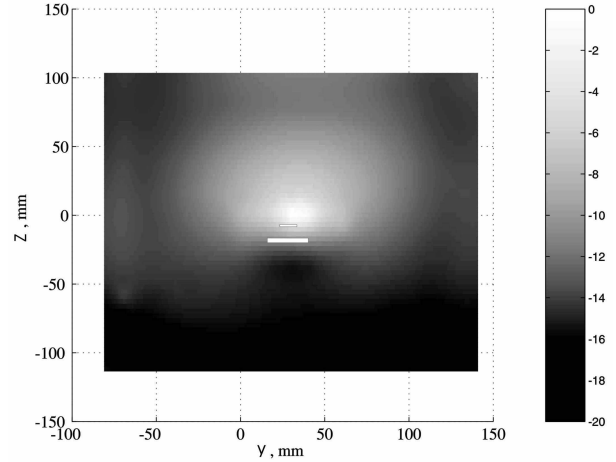


Fig. 5. Near-field spatial distribution in the vertical plane across the horizontally positioned folded half-dipole located over the mushroom impedance screen (electric field vector relative magnitude, dB). The antenna and the ground plane location are shown. The picture top corresponds to the region in front of the antenna, the bottom represents the screened area. The antenna structure is located in the region  $0 < y < 70 \text{ mm}$ ,  $-40 \text{ mm} < z < 0$ .

To compare the radiation properties of the studied antennas measurements of antenna impedances and antenna efficiencies have been done. The input impedance measurements have been performed with the HP 8753D network analyzer. To measure the efficiency, the antenna samples were covered by a conducting semi-sphere (Wheeler's cap), and the real part of the input impedance was measured. Then, the efficiency value was calculated as

$$\eta = (1 - R_0/R) \cdot 100\% \quad (5)$$

where  $R_0$  is the real part of the input impedance of the covered antenna at resonance, and  $R$  is the real part of the antenna impedance without the covering, at the resonance. The results of measurements are given in Table II. The best efficiency was achieved with the Jerusalem crosses structure. But in the same time this structure was the thickest one (see Table I).

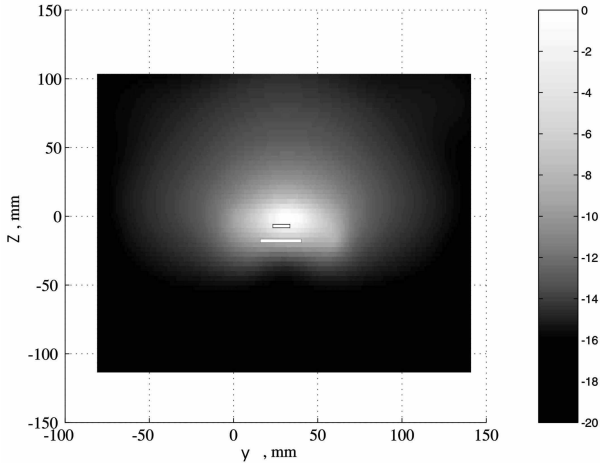


Fig. 6. The same as in Figure 5 for the magnetic field relative magnitude, dB.

TABLE II

WHEELER-CAP ANTENNA EFFICIENCY MEASUREMENT RESULTS FOR THE ANTENNAS UNDER TEST.

	Mushrooms	Metal	Jerusalem crosses
$R$ , Ohm	22	25	25
$R_0$ , Ohm	6	6	3
Efficiency, %	73	76	88

#### D. Some numerical results by the FDTD method

A three-dimensional computer code for the numerical calculation of the input antenna parameters has been developed. The FDTD method was used to solve the Maxwell equations in the time domain, the simulated data were converted into the frequency domain by the Fourier transform. The mushroom surface impedance was modeled as the input impedance of a parallel circuit with the parameters given by  $\tilde{m}$ s. For details of the simulation method, see [6]. In this example the distance of the dielectric support of the radiator from the impedance screen is 7.7 mm. The numerical and measured results for the magnitude of  $S_{11}$  parameter are presented in Figure 7. The smallest reflection occurs at about 1.9 GHz, in agreement with the measured results. So, the antenna is tuned as we need and has a rather good bandwidth for this frequency range (8% on the level  $-10$  dB).

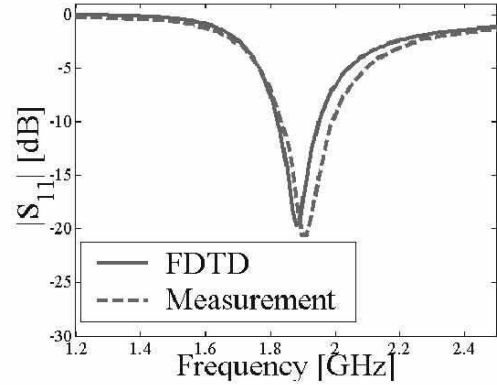


Fig. 7. The magnitude of  $S_{11}$  parameter of the folded dipole over the impedance surface. The measured and the simulated results agree relatively well.

### III. FULL-SIZED FOLDED DIPOLE AND A SYMMETRIZED PROTOTYPE ANTENNA

#### A. The prototype antenna

Experiments with the modeling set-up (Section II) have shown that there is a possibility to obtain a 50 Ohm (full-sized) matched antenna using the folded dipole placed on top of an impedance surface. The needed distance of the antenna from the impedance surface was found experimentally. When a real full-size antenna is fed by a coaxial cable, a symmetrizing device is needed. Such a device has been designed and manufactured using the planar technique. The photo is shown in Figure 8.

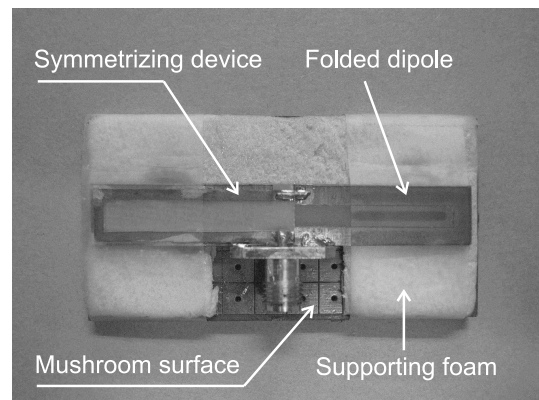


Fig. 8. The prototype folded-dipole antenna with an integrated symmetrizing device. Behind the antenna a foam layer and the mushroom surface are seen.

The folded dipole and the designed symmetrizing device are inseparable parts of a microstrip construction. The detailed chart of the construction is given in Figure 9. The developed

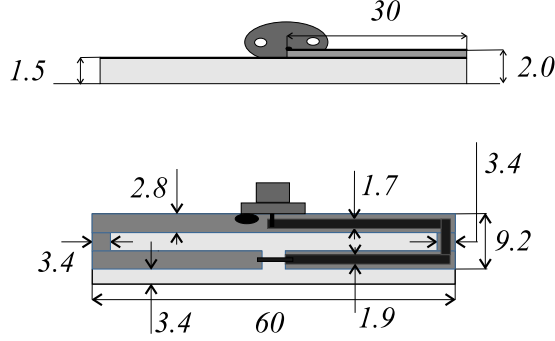


Fig. 9. A detailed chart of the developed folded-dipole antenna with an integrated symmetrizing device.

radiator is fed as follows. The outer connector of the coax is attached to the central point of one of the two conductors that form the folded dipole. The output voltage of the coaxial cable is transmitted to the feeding point by a microstrip line formed by an additional strip placed on top of one of the folded dipole conductors. If the width of the additional strip is smaller than the width of the dipole strip, and if the separation between the two strips is much smaller than the width of the folded dipole, the total construction radiates as a single folded dipole. That is because the additional strip is effectively screened by the dipole itself and does not influence the operation of the antenna. The construction is effectively symmetric, since the outer connector of the coaxial cable is attached to a zero-potential point. Moreover, the width of the additional conductor and the thickness of the insulator can be chosen so that the additional microstrip line is a 50 Ohm line. Alternatively, it is possible to use this transmission line segment as an impedance transformer, if the line characteristic impedance differs from 50 Ohm.

#### B. Near-field measurements with the prototype antenna

The prototype antenna consists of a balanced folded dipole over a mushroom layer of the size  $64 \times 33 \text{ mm}^2$ . The same measurement procedure as described in Section II was used

to measure the prototype antenna. The only difference in the set-up was that it had no additional metal screen and the cable was directly connected to the antenna. The location of the measurement points and the orientation of the prototype antenna under measurement are shown in Figure 10.

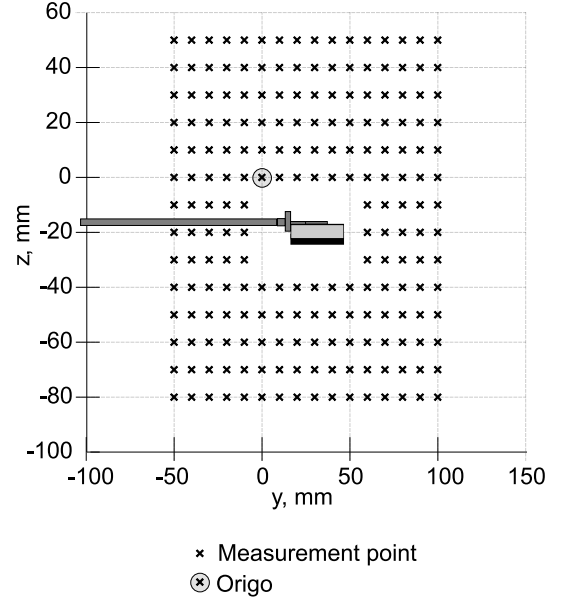


Fig. 10. The location of the measurement points and the orientation of the prototype antenna under measurement. The feeding coaxial cable is seen on the left.

Test field distributions along the antenna dipole showed that the antenna was well balanced. The operating frequency was 1.77 GHz. We have measured the field distribution around the antenna and calculated the averaged screening effect taking into account the field at every point shown in Fig. 10. The results depicted in Figures 11 and 12 are in good agreement with similar ones obtained in the first experiment with a half of an analogous antenna. A small asymmetry of the electric field distribution is caused by the coaxial cable connected to the dipole. The input return loss at the resonance is  $|S_{11}| = -20$  dB, the radiation efficiency is 73%, the averaged screening effect  $ASE = 13$  dB, the input resistance at the resonance is 61 Ohm, the antenna bandwidth at the level  $-6$  dB (for  $S_{11}$ ) is 9% (at  $-9.5$  dB it is 5.5%).

We also studied the same radiating element with other impedance surfaces behind it: Jerusalem-slot screen and a metal plate. In both these cases we obtained good agreement with the studies of the half of a similar folded dipole (Section II). The final results are presented in Table III.

TABLE III

MAIN PARAMETERS OF THE THREE DESIGNED PROTOTYPES.

	Metal plate	Mushrooms	Jerusalem crosses
Central frequency, GHz	1.81	1.77	1.83
Radiation efficiency <sup>†</sup> , %	76	73	88
Total thickness $H$ , mm	9.35	8.3	12.3
Bandwidth, %	–	5.5 (–9.5 dB)	4 (–10 dB)
Electric field ASE, dB	15	13	15
Magnetic field ASE, dB	15–17	12–13	13–15

<sup>†</sup> The efficiency values were measured in the modeling set-up discussed in Section II.

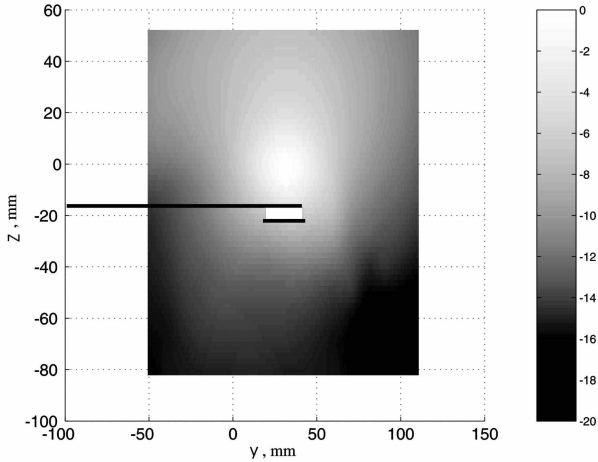


Fig. 11. Near-field spatial distribution of the prototype full-size folded dipole antenna around the radiating system. The electric field vector relative magnitude, is given in dB. The position of the antenna and feeding cable are shown. The radiating structure is located in region  $15 \text{ mm} < y < 45 \text{ mm}$ ,  $-25 \text{ mm} < z < -17 \text{ mm}$ , see Figure 10.

#### IV. CONCLUSIONS

Compared to the known designs of antennas utilizing high-impedance surfaces (see, e.g. [2], [8]), our prototypes are much superior in the screening effect. We do not know works

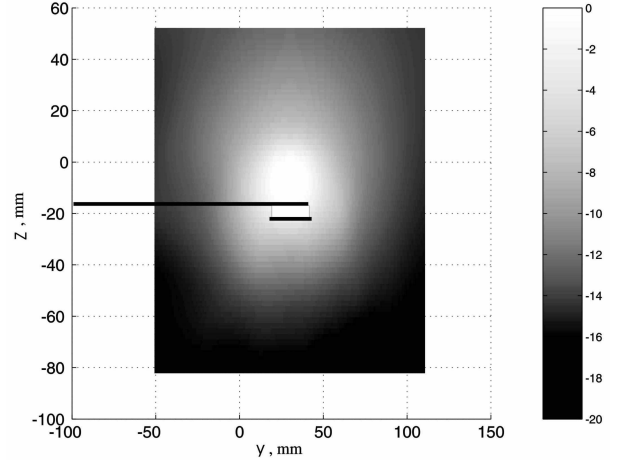


Fig. 12. The same as in Figure 11 for the magnetic field relative magnitude, dB.

in which the near-field screening effect would be calculated or measured for antennas operating at 1–3 GHz. In [8] the screening effect of 7 dB corresponds to the far-zone field, and in [2] 6 dB is the front-to-back ratio (also a far-zone parameter). To compare our results with the basic known ones we should replace ASE introduced in our paper by its analogue in which the far-zone part of our measured data is kept. Estimation of the distance to the far zone is not obvious in this case when the antenna is not electrically large but cannot be considered as a point source. Looking at the distance to the far-zone  $Z$  for considerably large antennas

$$Z = \frac{2G^2}{\lambda}, \quad (6)$$

where  $G = 64 \text{ mm}$  is the maximal size of our radiating system, and to the same for point dipoles

$$Z = \frac{\lambda}{2\pi} \quad (7)$$

and choosing the larger value, we estimate that the distance  $Z > 5 \text{ cm}$  from the antenna (which corresponds to the  $z$ -coordinates  $z = 35 \dots 50$  and  $z = -70 \dots -80 \text{ mm}$  in Fig. 10) can be referred to the far-zone. Calculating ASE for these distances we obtain 18 dB for the present design against the known 6–7 dB [2] and [7]. It is also clearly visible

in Figures 5, 6, 11, 12 that the maximal screening effect in our measurements corresponds to relatively large distances. Therefore, we assume that the result of 6 dB for the front-to-back ratio in the far zone corresponds to a practically small ASE for the near field and does not witness any considerable improvement of the near-field pattern of the antenna.

We also have demonstrated increased radiation efficiency (73-88 percent against the known 60 percent). However, the designs of [2], [8] have smaller thicknesses (approximately 3 mm against our 8-12 mm). Let us explain this point. We have tried to achieve a compromise between high near-field screening, high efficiency, and a small thickness with the emphasis on the near-field screening. Notice, that in other known designs, the resonant frequency region of the mushroom surface is used. In that regime the surface operates as a magnetic screen, which means that the radiating element can be brought very close to the surface without cancelation of the radiation resistance. This allows a compact design. But, this leads to a smaller screening efficiency [1]. And this point was not studied enough in the known literature.

Also, the radiation efficiency of an antenna over a high-impedance surface can be lower than in the regime of the moderate surface impedance because of stronger fields in the dielectric substrate. In our design we work at a frequency much lower than the impedance surface resonance. In this region the surface impedance is rather low, so that the properties are close to that of an *electric* screen. For this reason we cannot bring the primary radiator very close to the surface, and the thickness is increased, but the screening of the back radiation is very much improved. The bandwidth is the best for the case of the mushroom surface. The simple metal plate ( $Z_s \approx 0$ ) can be used for screening if we neglect the requirement of the broad band antenna operation (and allow even thicker design).

Summarizing, we can conclude that it has been experimentally demonstrated that simple artificial impedance surfaces

can be used in the design of antennas for reducing the near field behind the antenna and increasing the antenna efficiency without any bandwidth reduction.

#### ACKNOWLEDGMENT

This work was supported in part by Nokia Research Center, Filtronic LK, and TEKES.

#### REFERENCES

- [1] S.A. Tretyakov and C.R. Simovski, "Wire antennas near artificial impedance surfaces," *Microwave Opt. Tech. Lett.*, vol. 27, no. 1, pp. 46–50, 2000.
- [2] W.E. McKinzie and R.R. Fahr, "A low profile polarization diversity antenna built on an artificial magnetic conductor," *2002 IEEE Antennas Propag. Society International Symposium and USNC/URSI National Radio Science Meeting*, San Antonio, TX, USA, pp. 762–765, June 16–21, 2002.
- [3] D. Sievenpiper *et al.*, "High-impedance electromagnetic surfaces with a forbidden frequency band," *IEEE Trans. Microwave Theory Tech.*, vol. 47, pp. 2059–2074, 1999.
- [4] F.P. Yang, K.-P. Ma, Y. Qian, and T. Itoh, "A novel TEM waveguide using UC-PBG structures," *IEEE Trans. Microwave Theory Tech.*, vol. 47, pp. 2092–2098, 1999.
- [5] J.Y. Park, C.C. Chang, Y. Qian, and T. Itoh, "An improved low-profile cavity-backed slot antenna loaded with 2D UC-PBG reflector," *2001 IEEE Antennas Propag. Society International Symposium and USNC/URSI National Radio Science Meeting*, USA, vol. 4, pp. 194–197, June, 2001.
- [6] M. Kärkkäinen and S. Tretyakov, "2D-FDTD modeling of wire antennas near artificial impedance surfaces," *Microwave Opt. Tech. Lett.*, vol. 34, no. 1, pp. 38–40, 2002.
- [7] M. Vnuk and R. Kubacki, "Dual-band antenna and minimization of radiation towards head," *2004 Progress in Electromagnetics Research Symposium*, Italy, vol. 2, pp. 914–917, March, 2004.
- [8] J.J. Lee, R.J. Broas, and S. Livingston, "Flush-mounted antennas on Hi-Z ground planes," *2002 IEEE Antennas and Propagation Society International Symposium and USNC/URSI National Radio Science Meeting*, San Antonio, TX, USA, pp. 764–767, June 16–21, 2002.
- [9] S.A. Tretyakov and C.R. Simovski, "Dynamic model of artificial reactive impedance surfaces," *J. Electromagn. Waves Appl.*, vol. 17, no. 1, pp. 131–145, 2003.
- [10] I.H. Lindell, *Methods of Electromagnetic Fields Analysis*. Clarendon Press, UK, 1992.